

Proceedings of the ASME 2023
International Mechanical Engineering Congress and Exposition
IMECE2023

October 29-November 2, 2023, New Orleans, Louisiana

IMECE2023-113559

A DYNAMIC MODEL FOR UNDERWATER PROPULSION OF AN AMPHIBIOUS ROVER DEVELOPED FROM KANE'S METHOD

Brigid Donohue, Sumedh Beknalkar, Matthew Bryant, Andre Mazzoleni

North Carolina State University, Raleigh, NC

ABSTRACT

The Multi-terrain Amphibious ARCtic explOrer (MAARCO) rover is an amphibious arctic rover designed to traverse arctic terrains and propel through water. The MAARCO rover consists of an ellipsoid chassis with links connecting to the propulsion system. The propulsion system consists of two helical drives made up of hollow cylinder ballasts wrapped in auger or screw shaped blades in opposing helical directions parallel to each other. In this paper, a 6 degree of freedom dynamic model of the MAARCO rover is created using Kane's method dynamic modeling to demonstrate the dynamic model capabilities for an underwater vehicle's performance. The hydrodynamic forces considered on the underwater rover include drag, buoyancy, flow acceleration, and added mass. In addition to the hydrodynamic forces the rover will experience gravity forces, control forces, net thrust from the helical drive blades, and net buoyancy from the helical drive ballast system. The equations of motion are developed from Kane's method to reduce computational cost and simulated in MATLAB for different cases to gain further understanding and provide a visual representation of the system underwater and the dynamic models capabilities. The results of the simulations show the MAARCO rover behavior in the hydrodynamic environment. The results reveal that the Kane's method dynamic modeling successfully develops equations of motion of a complicated system that can be implemented into a control system.

Keywords: Dynamic Model, Kane's Method, Hydrodynamic Forces, Kinematics, Underwater Vehicle, Amphibious Rover, Modeling and Simulation

1. INTRODUCTION

Exploration in the arctic region has become increasingly important in understanding the effects of global warming. The harsh environments in the arctic limit exploration capabilities, and autonomous vehicles can provide more opportunities to explore these regions that are otherwise dangerous or inaccessible

Documentation for asmeconf.cls: Version 1.34, July 31, 2023.

to human-led missions. Underwater rovers provide additional exploration capabilities to further study the arctic bodies of water.

The Multi-terrain Amphibious ARCtic explOrer (MAARCO) rover is an amphibious arctic rover capable of traversing across different terrains and propelling through water [1] [2] [3] [4] [5]. The MAARCO rover propulsion system is made up of two hollow cylinder ballasts wrapped in auger or screw shaped blades in opposing helical directions parallel to each other, referred to as helical drives. When operating as an underwater vehicle the helical drive blades provide thrust as the helical drives rotate and the hollow cylinder ballast system adjusts the buoyancy of the rover as water is filled or drained.

A dynamic model of an underwater rover is necessary to provide an understanding of the vehicle's performance in the underwater environment and simulate the motion of the rover. The dynamic model is essential in evaluating the vehicle's performance under different conditions and will provide information considered in the rover design parameters, controls strategies, and overall mission operations. Underwater robotic vehicles (URV) have limited studies done on them because of uncertainties with hydrodynamic forces, where the model requirements of the URV include a model based dynamic control system, the vehicle, and the dynamic system in an underwater environment [6].

In this paper, a dynamic model of the MAARCO rover is created using Kane's method dynamic modeling to create a simplified model for a complicated underwater vehicle system. The dynamic model considers the rover system model and the underwater environment interactions with the system. The model monitors the generalized coordinates of the 6 degree-of-freedom rover with hydrodynamic forces acting on the rover and is used to simulate the response of the rover in different cases.

2. KANE'S METHOD BACKGROUND

Kane's Method is a dynamic modeling method used for calculating the equations of motion for a system that uses generalized speeds, partial velocities, and partial angular velocities in generalized active force and generalized inertia force equations to develop the equations of motion [7]. The system is described in terms of $q_1, ...q_r$ generalized coordinates, and $\dot{q}_1, ...\dot{q}_r$ generalized velocities. Kane's method expresses the equations of motion in $u_1, ...u_r$ generalized speeds that are developed from the generalized velocities to create equations that describe the vehicle's motion and simplify the model [7].

$$[u] = [Y][\dot{q}] - [Z]$$
 (1)

The only requirements of the generalized speeds is that they are able to solve unique expressions for the generalized velocities [7]. Therefore [Y] must have an inverse, [W], that exists and can be used to calculate the generalized velocities.

$$[\dot{q}] = [W][u] + [Z][u]$$
 (2)

These generalized speed equations result in 2r first order differential equations, $\dot{q}_1,...\dot{q}_r$ and $\dot{u}_1,...\dot{u}_r$. As opposed to r second order differential equations, $\ddot{q}_1,...\ddot{q}_r$, that would be found in models using Newton-Euler and Lagrange methods. This results in simplified equations and lower computational efforts.

The Kane's Method equation is $F_r + F_r^* = 0$ where the generalized active force, F_r , is

$$F_{r} = \sum_{k=1}^{N_{R}} (\vec{F}_{k} \cdot {}_{O}^{\vec{O}} \vec{v}_{cm_{k},r} + \vec{\tau}_{cm_{k},r} \cdot {}_{O}^{\vec{O}} \vec{\omega_{r}}^{\vec{B}_{k}}) + \sum_{l=1}^{N_{P}} \vec{f}_{l} \cdot {}_{O}^{\vec{O}} \vec{v}_{m_{l},r}$$
(3)

And the generalized inertia force $F_r *$ is

$$F_r^* = -\sum_{k=1}^{N_R} (m_k{}^{\bar{o}} \vec{a}_{cm_k/O} \cdot {}^{\bar{o}}_o \vec{v}_{cm_k,r} + ((\tilde{I}_{cm_k} \cdot {}^{\bar{O}} \vec{\alpha}^{\bar{B}_k} +$$

$${}^{\bar{O}}\vec{\omega}^{\bar{B}_{\bar{k}}} \times (\tilde{I}_{cm_k} \cdot {}^{\bar{O}}\vec{\omega}^{\bar{B}_{\bar{k}}})) \cdot {}^{\bar{O}}\vec{\omega}_r^{\bar{B}_{\bar{k}}}) - \sum_{l=1}^{N_P} m_l {}^{\bar{O}}\vec{a}_{m_l/O} \cdot {}^{\bar{O}}\vec{v}_{m_l,r} \quad (4)$$

Where r is the r^{th} generalized speed, N_R is the number of rigid bodies in a system, and $\bar{B_k}$ is the body frame of the k^{th} rigid body. For a rigid body, the velocities and angular velocities are

$${}^{\bar{O}}\vec{v}_{cm_k/O} = \sum_{r=1}^{n} ({}^{\bar{O}}_{O}\vec{v}_{cm_k,r} * u_r) + {}^{\bar{O}}_{O}\vec{v}_{cm_k,t}$$
 (5)

$${}^{\bar{O}}\vec{\omega}^{\bar{B}_{k}} = \sum_{r=1}^{n} ({}^{\bar{O}}\vec{\omega_{r}}^{\bar{B}_{k}} * u_{r}) + {}^{\bar{O}}\vec{\omega_{t}}^{\bar{B}_{k}}$$
 (6)

where n is the number of general coordinates. ${}^{\bar{O}}_{C}\vec{v}_{cm_k,r}$ is the r^{th} partial velocity and ${}^{\bar{O}}\vec{\omega_r}^{\bar{B}_k}$ is the r^{th} partial angular velocity. From inspection the partial velocities and partial angular velocities can be calculated by

$${}_{O}^{\bar{O}}\vec{v}_{cm_{k},r} = \frac{\partial}{\partial u_{r}}{}^{\bar{O}}\vec{v}_{cm_{k}/O} \tag{7}$$

$${}^{\bar{O}}\vec{\omega_r}{}^{\bar{B_k}} = \frac{\partial}{\partial u_r}{}^{\bar{O}}\vec{\omega}^{\bar{B_k}} \tag{8}$$

And where N_P is the number of point masses, or particles, in a system with l particles in the system. For a particle, the velocity is

$${}^{\bar{O}}\vec{v}_{m_l/O} = \sum_{r=1}^{n} ({}^{\bar{O}}_{O}\vec{v}_{m_l,r} * u_r) + {}^{\bar{O}}_{O}\vec{v}_{m_l,t}$$
 (9)

where n is the number of general coordinates. ${}^{\bar{O}}_{O}\vec{v}_{m_l,r}$ is the r^{th} partial velocity. From inspection the partial velocity is calculated by

$${}_{O}^{\bar{O}}\vec{v}_{m_{l},r} = \frac{\partial}{\partial u_{r}}{}^{\bar{O}}\vec{v}_{m_{l}/O} \tag{10}$$

3. ROVER MODEL

3.1 Rover Description

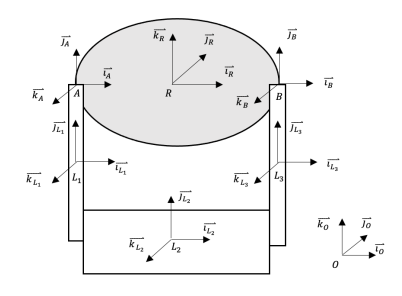
The rover is designed to traverse through the arctic terrain in substrates such as ice, mud, dirt, and water. The structure of the rover contains a rover chassis and robotic arms to position the helical drives, as well as controlled sliding masses located within the rover chassis. The helical drive position adjusts the maneuver capabilities of the rover in varying conditions, and is controlled by an applied position or motion. For example having the helical drives underneath the chassis to help traverse across terrain or positioning them to the side parallel with the chassis to propel through water to reduce involuntary pitching from the resulting torque of thrust acting beneath the rover chassis and drag acting on the rover chassis. The rover chassis is currently modeled as an ellipsoid to provide a more streamlined shape for underwater purposes. The sliding masses provide additional force control for the motion of the rover. The underwater dynamics of the helical drives is largely unknown and will be modeled as cylinders in the current system with forces from the helical drives acting on the body.

3.2 Rover System Coordinates

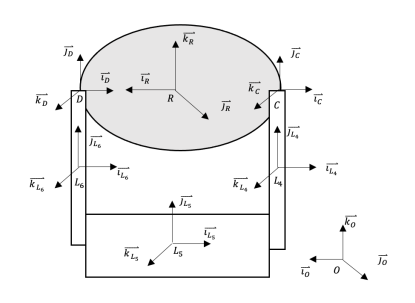
The rover body connects to the links supporting the helical drive propulsion system. The rover body, links, and helical drives each have a body frame that is attached and rotates with the body. The body frames are relative to the inertial reference frame of the system, assumed to be Earth. The body frame of the rover chassis \bar{R} , is located at the rover chassis center of mass R and is $\bar{R} = \{R, \vec{i}_{\bar{R}}, \vec{j}_{\bar{R}}, \vec{k}_{\bar{R}}\}$. Where b is the semi-major axis of the rover chassis and a is the semi-minor axis of the rover chassis. The arms are represented in 4 links (L_1, L_3, L_4, L_6) and the helical drives are modeled as cylinders (L_2, L_5) . These are the rigid bodies of the system with body frames \bar{L}_1 , \bar{L}_2 , \bar{L}_3 , \bar{L}_4 , \bar{L}_5 , and \bar{L}_6 located at the bodies center of mass L_1 , L_2 , L_3 , L_4 , L_5 , and L_6 . The link and helical drive body frames are $\bar{L}_1 = \{L_k, \bar{i}_{L_k}, \bar{j}_{L_k}, \bar{k}_{L_k}\}$.

The inertial reference frame \bar{O} is attached to Earth at the Earth center of mass O and is $\bar{O} = \{O, \vec{i}_{\bar{O}}, \vec{j}_{\bar{O}}, \vec{k}_{\bar{O}}\}.$

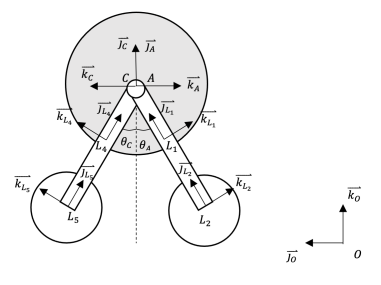
The links are connected to hinges A, B, C, and D at the major axis poles of the ellipsoid which allow rotation in the link body \vec{j} - \vec{k} plane. The body frames are displayed in Fig. 1. The arm links and helical drive drive system rotate an angle θ_A , θ_B , θ_C , and θ_D about the hinges A, B, C, and D as shown in Fig. 1. θ_A and θ_B are assumed to be equal, because the arms are all connected to each other with no change in position relative to each link unless there is a structural failure. θ_C and θ_D are assumed to be equal, because the arms are all connected to each other with no change in position



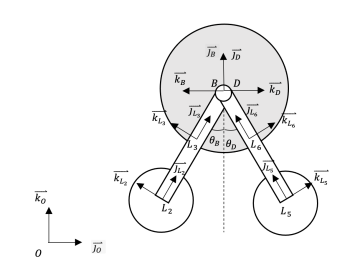
(a) A-B Side Body Frames



(b) C-D Side Body Frames



(c) Front View Body Frames



(d) Back View Body Frames

FIGURE 1: ROVER SYSTEM FRAMES

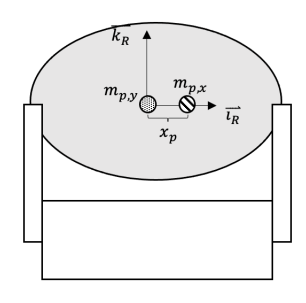


FIGURE 2: SIDE VIEW OF ROVER WITH SLIDING MASSES

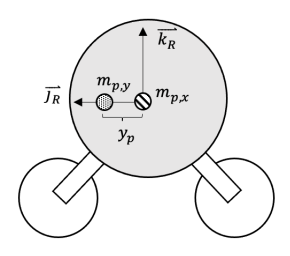


FIGURE 3: FRONT VIEW OF ROVER WITH SLIDING MASSES

relative to each link unless there is a structural failure. The hinge reference frames are $\bar{A}=\{A,\vec{i}_{\bar{A}},\vec{j}_{\bar{A}},\vec{k}_{\bar{A}}\},\;\bar{B}=\{B,\vec{i}_{\bar{B}},\vec{j}_{\bar{B}},\vec{k}_{\bar{B}}\},\;\bar{C}=\{C,\vec{i}_{\bar{C}},\vec{j}_{\bar{C}},\vec{k}_{\bar{C}}\},\bar{D}=\{D,\vec{i}_{\bar{D}},\vec{j}_{\bar{D}},\vec{k}_{\bar{D}}\}.$

The dimensions of the links and helical drives are l_1 =length of link 1, d_1 = diameter of link 1, d_2 = diameter of link 2, l_3 = length of the drive, d_3 = diameter of the drive, l_4 = length of link 4, d_4 = diameter of link 4, l_5 = length of link 5, and d_5 = diameter of link 5, l_6 = length of link 6, d_6 = diameter of link 6. The sliding masses inside of the rover chassis adjust the orientation of the rover body and allow more pitch and roll control. The sliding masses are modeled as point masses that move within the enclosed rover chassis in the rover body frame with an applied and known motion. The x-direction point mass $m_{p,x}$ will be able to move forward and backward in the \vec{l}_R direction as shown in Fig. 2. The y-direction point mass $m_{p,y}$ will be able to move side to side in the \vec{l}_R direction as shown in Fig. 3.

3.3 Mass and Moment of Inertia

The mass of the sliding masses are $m_{p,x}$ for the x-direction point mass and $m_{p,y}$ for the y-direction point mass. The masses of each of the links and helical drives are m_1, m_2, m_3, m_4, m_5 . The mass of the rover body is m_{rov} . The moment of inertia for the links and helical drives are modeled as thin rods. The moment of inertia for the rover chassis is modeled as an ellipsoid. The mass moment of inertia for each link (L_1, L_3, L_4, L_6) about each link center of mass, approximated as a thin rod, is

$$\tilde{I}_{cm_k} = \left[\frac{1}{12} m_k l_k^2 \right] \vec{i}_{\bar{L}_k} \vec{i}_{\bar{L}_k} + [0] \vec{j}_{\bar{L}_k} \vec{j}_{\bar{L}_k} + \left[\frac{1}{12} m_k l_k^2 \right] \vec{k}_{\bar{L}_k} \vec{k}_{\bar{L}_k}$$

The mass moment of inertia for each helical drive (L_2, L_5) about each helical drive center of mass, approximated currently as a thin rod, is

$$\tilde{I}_{cm_k} = [0] \, \vec{i}_{\bar{L}_k} \, \vec{i}_{\bar{L}_k} + \left[\frac{1}{12} m_k l_k^2 \right] \, \vec{j}_{\bar{L}_k} \, \vec{j}_{\bar{L}_k} + \left[\frac{1}{12} m_k l_k^2 \right] \, \vec{k}_{\bar{L}_k} \, \vec{k}_{\bar{L}_k}$$

The mass moment of inertia for the rover chassis (R) about the rover chassis center of mass is

$$\begin{split} \tilde{I}_{R} &= \left[\frac{1}{5}m_{rov}(a^{2}+a^{2})\right]\vec{i}_{R}\vec{i}_{\bar{R}} + \left[\frac{1}{5}m_{rov}(a^{2}+b^{2})\right]\vec{j}_{\bar{R}}\vec{j}_{\bar{R}} \\ &+ \left[\frac{1}{5}m_{rov}(a^{2}+b^{2})\right]\vec{k}_{\bar{R}}\vec{k}_{\bar{R}} \end{split}$$

3.4 Kinematics

The kinematic expressions of the rover describe the translational and rotational motion of the rover system without respect to the forces [7]. The direction cosine matrices are defined to show the rotation between different frames in the system and can be used to calculate the angular velocities and angular accelerations between frames. The position vectors describe the location of the rigid bodies and particles, and can be used to calculate the velocities and accelerations of between points.

The direction cosine matrix between \bar{R} and \bar{O} will follow NASA Standard order yaw (ψ) , pitch (θ) , then roll (ϕ) .

$${}^{\bar{R}}[C]^{\bar{O}} = [R_x(\phi)][R_v(\theta)][R_z(\psi)] \tag{11}$$

The angular velocity between the rover chassis body frame \bar{R} and the inertial reference frame \bar{O} can be calculated from the direction cosine matrices ${}^{\bar{R}}[C]^{\bar{O}}$.

$${}^{\bar{O}}\vec{\omega}^{\bar{R}} = {}^{\bar{O}}\omega_x{}^{\bar{R}}\vec{i}_{\bar{R}} + {}^{\bar{O}}\omega_y{}^{\bar{R}}\vec{j}_{\bar{R}} + {}^{\bar{O}}\omega_z{}^{\bar{R}}\vec{k}_{\bar{R}}$$
(12)

$${}^{\bar{O}}\omega_x{}^{\bar{R}} = \begin{bmatrix} 0 & 0 & 1 \end{bmatrix} {}^{\bar{R}} [C]^{\bar{O}\bar{O}} [\dot{C}]^{\bar{R}} \begin{bmatrix} 0 \\ 1 \\ 0 \end{bmatrix}$$
 (13)

$${}^{\bar{O}}\omega_{y}{}^{\bar{R}} = \begin{bmatrix} 1 & 0 & 0 \end{bmatrix}{}^{\bar{R}} [C]^{\bar{O}\bar{O}} [\dot{C}]^{\bar{R}} \begin{vmatrix} 0 \\ 0 \\ 1 \end{vmatrix}$$
 (14)

$${}^{\bar{O}}\omega_z{}^{\bar{R}} = \begin{bmatrix} 0 & 1 & 0 \end{bmatrix}{}^{\bar{R}} [C]^{\bar{O}\bar{O}} [\dot{C}]^{\bar{R}} \begin{bmatrix} 1 \\ 0 \\ 0 \end{bmatrix}$$
 (15)

The angular acceleration vectors of the rover chassis body frame is calculated from the time derivative of the angular velocity vector.

$${}^{\bar{O}}\vec{\alpha}^{\bar{R}} = {}^{\bar{O}}\frac{d}{dt}{}^{\bar{O}}\vec{\omega}^{\bar{R}} \tag{16}$$

The direction cosine matrices for the hinge, link, and helical drive frames for the current rover design are defined in Appendix A and can be used to calculate the angular velocity and angular acceleration of each rigid body.

The position vector for the rover chassis body is a function of time and can be used to calculate the velocity and acceleration vector of the rover chassis body.

$$\vec{r}_{R/O} = x\vec{i}_{\bar{O}} + y\vec{j}_{\bar{O}} + z\vec{k}_{\bar{O}}$$
 (17)

Where x, y, and z are functions of time.

The velocity vector of of the rover body from the inertial reference frame is calculated from the position vector.

$$\bar{O}_{R/O} = \bar{O}\frac{d}{dt}\vec{r}_{R/O} = \bar{R}\frac{d}{dt}\vec{r}_{R/O} + \bar{O}\omega^{\bar{R}}\times\vec{r}_{R/O}$$
 (18)

The acceleration vector of of the rover body from the inertial reference frame is calculated from the velocity vector.

$${}^{\bar{O}}\vec{a}_{R/O} = {}^{\bar{O}}\frac{d}{dt}{}^{\bar{O}}\vec{v}_{R/O} = {}^{\bar{R}}\frac{d}{dt}{}^{\bar{O}}\vec{v}_{R/O} + {}^{\bar{O}}\omega^{\bar{R}} \times {}^{\bar{O}}\vec{v}_{R/O}$$
(19)

The position vector for the x-direction point mass particle, $m_{p,x}$, from the rover chassis center of mass is

$$\vec{r}_{m_{p,x}/R} = x_p \vec{i}_{\bar{R}} + 0 \vec{j}_{\bar{R}} + 0 \vec{k}_{\bar{R}}$$
 (20)

Where x_p , is a function of time.

The position vector for the y-direction point mass particle, $m_{p,y}$, from the rover chassis center of mass is

$$\vec{r}_{m_{p,y}/R} = 0\vec{i}_{\bar{R}} + y_p \vec{j}_{\bar{R}} + 0\vec{k}_{\bar{R}}$$
 (21)

Where y_p , is a function of time.

The position vectors between the link and helical drive center of masses to the inertial reference frame for the current rover design are defined in Appendix B and can be used to calculate the velocity and acceleration at the center of mass for each rigid body.

3.5 Rover System Kane's Method

3.5.1 Generalized Speeds. The generalized coordinates of the rover system are

 $q_1 = x$ - the position of R relative to O in $\vec{i}_{\bar{O}}$ $q_2 = y$ - the position of R relative to O in $\vec{j}_{\bar{O}}$ $q_3 = z$ - the position of R relative to O in $\vec{k}_{\bar{O}}$ $q_4 = \phi$ - roll of \bar{R} relative to \bar{O} in $\vec{i}_{\bar{O}}$ $q_5 = \theta$ - pitch of \bar{R} relative to \bar{O} in $\vec{k}_{\bar{O}}$ $q_6 = \psi$ - yaw of \bar{R} relative to \bar{O} in $\vec{j}_{\bar{O}}$

The time derivatives of the generalized coordinates return the generalized velocities.

$$\dot{q}_1 = \dot{x}$$

$$\dot{q}_2 = \dot{y}$$

$$\dot{q}_3 = \dot{z}$$

$$\dot{q}_4 = \dot{\phi}$$

$$\dot{q}_5 = \dot{\theta}$$

$$\dot{q}_6 = \dot{\psi}$$

The generalized speeds for the system are selected to be

$$u_1 = v_x$$

$$u_2 = v_y$$

$$u_3 = v_z$$

$$u_4 = \omega_x$$

$$u_5 = \omega_y$$

$$u_6 = \omega_z$$

Where v_x , v_y , and v_z are the x, y, and z velocities of the rover expressed in the \bar{R} frame relative to the inertial reference frame.

$$\{{}^{\bar{O}}\vec{v}_{R/O}\}_{\bar{R}} = v_x \vec{i}_{\bar{R}} + v_y \vec{j}_{\bar{R}} + \dot{z} \vec{k}_{\bar{R}}$$

This direction cosine matrices is used to relate $\{{}^{\bar{O}}\vec{v}_{R/O}\}_{\bar{O}}$ and $\{{}^{\bar{O}}\vec{v}_{R/O}\}_{\bar{R}}$

$$\{^{\bar{O}}\vec{v}_{R/O}\}_{\bar{O}}=\dot{x}\vec{i}_{\bar{O}}+\dot{y}\vec{j}_{\bar{O}}+v_z\vec{k}_{\bar{O}}$$

$$\{{}^{\bar{O}}\vec{v}_{R/O}\}_{\bar{R}} = {}^{\bar{R}} [C]^{\bar{O}} \{{}^{\bar{O}}\vec{v}_{R/O}\}_{\bar{O}}$$

The velocity equations are

$$v_x = \dot{x}\cos\theta\cos\psi + \dot{y}\cos\theta\sin\psi - \dot{z}\sin\theta$$

$$v_y = \dot{x}(\cos\psi\sin\phi\sin\theta - \cos\phi\sin\psi) + \dot{y}(\cos\phi\cos\psi$$

 $+\sin\phi\sin\theta\sin\psi) + \dot{z}\cos\theta\sin\phi$

 $v_7 = \dot{x}(\cos\phi\cos\psi\sin\theta + \sin\phi\sin\psi) + \dot{y}(-\cos\psi\sin\phi)$

 $+\cos\phi\sin\theta\sin\psi) + \dot{z}\cos\phi\cos\theta$

The ω_x , ω_y , and ω_z are the x, y, and z angular velocities of the rover expressed in the \bar{R} frame relative to the inertial reference frame.

$$\bar{O}\vec{\omega}^{\bar{R}} = \omega_x \vec{i}_{\bar{R}} + \omega_y \vec{j}_{\bar{R}} + \omega_z \vec{k}_{\bar{R}}$$

$$\omega_x = \begin{bmatrix} 0 & 0 & 1 \end{bmatrix}^{\bar{R}} \begin{bmatrix} C \end{bmatrix}^{\bar{O}\bar{O}} \begin{bmatrix} \dot{C} \end{bmatrix}^{\bar{R}} \begin{bmatrix} 0 \\ 1 \\ 0 \end{bmatrix}$$

$$\omega_{\mathbf{y}} = \begin{bmatrix} 1 & 0 & 0 \end{bmatrix}^{\bar{R}} \begin{bmatrix} C \end{bmatrix}^{\bar{O}\bar{O}} \begin{bmatrix} \dot{C} \end{bmatrix}^{\bar{R}} \begin{bmatrix} 0 \\ 0 \\ 1 \end{bmatrix}$$

$$\omega_z = \begin{bmatrix} 0 & 1 & 0 \end{bmatrix}^{\bar{R}} \begin{bmatrix} C \end{bmatrix}^{\bar{O}\bar{O}} [\dot{C}]^{\bar{R}} \begin{bmatrix} 1 \\ 0 \\ 0 \end{bmatrix}$$

The angular velocity equations are

$$\omega_x = \dot{\phi} - \dot{\psi} \sin \theta$$

$$\omega_{y} = \dot{\theta}\cos\phi - \dot{\psi}\cos\theta\sin\phi$$

$$\omega_z = \dot{\theta}\sin\phi - \dot{\psi}\cos\theta\cos\phi$$

The generalized speeds, or motion variables, u_r , are related to the generalized velocities through $[u] = [Y][\dot{q}] - [Z]$.

$$u_{1} = \dot{q}_{1}\cos q_{5}\cos q_{6} - \dot{q}_{3}\sin q_{5} + \dot{q}_{2}\cos q_{5}\sin q_{6}$$

$$u_{2} = \dot{q}_{3}\cos q_{5}\sin q_{4} + \dot{q}_{1}(\cos q_{6}\sin q_{4}\sin q_{5} - \cos q_{4}\sin q_{6}) + \dot{q}_{2}(\cos q_{4}\cos q_{6}) + \sin q_{4}\sin q_{5}\sin q_{6}) + \dot{q}_{2}(\cos q_{4}\cos q_{6}) + \sin q_{4}\sin q_{5}\sin q_{6})$$

$$u_{3} = \dot{q}_{3}\cos q_{5}\cos q_{4} + \dot{q}_{1}(\cos q_{6}\cos q_{4}\sin q_{5} + \sin q_{4}\sin q_{6}) + \dot{q}_{2}(-\sin q_{4}\cos q_{6} + \cos q_{4}\sin q_{5}\sin q_{6})$$

$$u_{4} = \dot{q}_{4} - \dot{q}_{6}\sin q_{5}$$

$$u_{5} = \dot{q}_{5}\cos q_{4} - \dot{q}_{6}\cos q_{5}\sin q_{4}$$

$$u_{6} = \dot{q}_{5}\sin q_{4} - \dot{q}_{6}\cos q_{5}\cos q_{4}$$

Then $[\dot{q}] = [W][u] + [Z][u]$ where [W] is the inverse of [Y] and [Z] = [0]. This returns \dot{q} values in terms of values u.

$$\dot{q}_1 = u_1 \cos q_5 \cos q_6 + u_2(\cos q_6 \sin q_4 \sin q_5 - \cos q_4 \sin q_6) + u_3(\cos q_4 \cos q_6 \sin q_5 + \sin q_4 \sin q_6)$$

$$\dot{q}_2 = u_1 \cos q_5 \sin q_6 + u_3(-\cos q_6 \sin q_4 + \cos q_4 \sin q_5 \sin q_6) + u_2(\cos q_4 \cos q_6 + \sin q_4 \sin q_5 \sin q_6)$$

$$\dot{q}_3 = u_3 \cos q_4 \cos q_5 + u_2 \cos q_5 \sin q_4 - u_1 \sin q_5$$

$$\dot{q}_4 = u_4 + u_6 \cos q_4 \tan q_5 + u_5 \sin q_4 \tan q_5$$

$$\dot{q}_5 = u_5 \cos q_4 - u_6 \sin q_4$$

$$\dot{q}_6 = u_6 \cos q_4 \sec q_5 + u_5 \sec q_5 \sin q_4$$

These 6 generalized speeds result in 6 governing Kane's method equations $F_r + F_r^* = 0$, one for each of the generalized speeds, $u_1, ... u_6$.

$$F_1 + F_1^* = 0$$

$$F_2 + F_2^* = 0$$

$$F_3 + F_3^* = 0$$

$$F_4 + F_4^* = 0$$

$$F_5 + F_5^* = 0$$

$$F_6 + F_6^* = 0$$

3.5.2 Partial Velocities and Partial Angular Velocities.

The velocities, angular velocities, accelerations, and angular accelerations are rewritten in terms of generalized coordinates $(q_1,...,q_6)$, the generalized speeds $(u_1,...,u_6)$, and the time derivative of the generalized speeds $(\dot{u}_1,...,\dot{u}_6)$. The partial velocities for the rigid bodies, ${}^{\bar{O}}_{\bar{V}cm_k,r}$, can be calculated from ${}^{\bar{O}}_{\bar{V}cm_k/O}$ for the 6 generalized speeds. The partial angular velocities for the rigid bodies, ${}^{\bar{O}}_{\bar{W}_r}{}^{\bar{B}_k}$, can be calculated from ${}^{\bar{O}}_{\bar{W}_{\bar{K}}}{}^{\bar{B}_{\bar{K}}}$ for the 6 generalized speeds. The partial velocities for the particles, ${}^{\bar{O}}_{\bar{O}}_{\bar{V}m_l,r}$, can be calculated from ${}^{\bar{O}}_{\bar{W}_{m_l/O}}$ for the 6 generalized speeds.

3.6 Forces

3.6.1 Calculating Link Forces. The forces acting on the links are approximated as point forces acting at the center of mass. The forces include gravity force $(\vec{F}_{k,grav})$, buoyancy force $(\vec{F}_{k,B})$, drag force $(\vec{F}_{k,drag})$, and flow acceleration force $(\vec{F}_{k,FA})$. There are also reaction forces at each the hinges and each link connection $(\vec{F}_{k,reaction})$. Assuming a frictionless system $(\vec{F}_{k,friction})$ is ignored. Also assuming that the vehicle is slow moving, lift $(\vec{F}_{k,lift})$ is ignored [6]. The forces acting on links 1, 3, 4, and 6 are

$$\vec{F}_k = \vec{F}_{k,grav} + \vec{F}_{k,B} + \vec{F}_{k,drag} + \vec{F}_{k,FA} + \vec{F}_{k,reaction}$$
 (22)

The links 2 and 5 have additional helical drive forces $(\vec{F}_{k,HD})$. Including a net thrust $(\vec{F}_{k,thrustnet})$ from the helical drive blades and a net buoyancy $(\vec{F}_{k,buoynet})$ from the helical drive ballast system that will fill and drain. The total forces for the links 2 and 5 are

$$\vec{F}_{k} = \vec{F}_{k,grav} + \vec{F}_{k,B} + \vec{F}_{k,drag} + \vec{F}_{k,FA} + \vec{F}_{k,reaction} + \vec{F}_{k,HD}$$
 (23)

Where $\vec{F}_{k,HD} = \vec{F}_{k,thrustnet} + \vec{F}_{k,buoynet}$ for links 2 and 5 only. The net thrust represents the net thrust from the helical drive rotation, and is the resulting thrust force remaining considering any drag forces opposing the rotation and forward movement. The net buoyancy force is the buoyancy from the ballast system inside of the helical drives to navigate the helical drive to rise or sink. These forces are unknown and applied as variables for this dynamic model. The thrust estimations can come from computational fluid dynamics simulations for helical drives [4]. The buoyancy from the ballast system can come from a ballast design and study.

The gravity forces acting on each link and helical drive are

$$\vec{F}_{k,grav} = m_k(-g)\vec{k}_{\bar{o}} \tag{24}$$

The buoyancy forces acting on the links and helical drives are proportional with the fluid that the links and helical drives displace acting through the center of buoyancy for each rigid body [6]. The center of buoyancy is assumed to be equal to the center of mass due to the symmetry of the rigid bodies present in the system. The buoyancy force acting on the link and the helical drives in the inertial reference frame, opposing the gravity force, is [6]

$$\vec{F}_{k,B} = -\rho V_k(-g)\vec{k}_{\bar{o}} \tag{25}$$

Where ρ is the density of the water and V_k is the volume of the fluid displaced by body k, which is approximated as the volume of each of the links as cylinders.

$$V_k = \pi r_k^2 l_k$$

The drag force acting on each link and helical drive is integrated across the length of the body [6].

$$\vec{F}_{k,drag} = -\frac{1}{2}\rho \int_0^{l_k} |\Delta^{\bar{O}} \vec{v}_{k,\perp}| \Delta^{\bar{O}} \vec{v}_{k,\perp} C_D r_k dl_k \qquad (26)$$

The drag force is simplified to a point force at the center of mass of each link

$$F_{k,drag} = -\frac{1}{2}\rho C_D |\Delta^{\bar{O}} \vec{v}_{k,\perp}| \Delta^{\bar{O}} \vec{v}_{k,\perp} S_k \tag{27}$$

Where S_k is the reference area of the body. The reference area for a cylinder is $S_k = r_k l_k$. $\Delta^{\bar{O}} \vec{v}_k$ is the difference between the link velocity $(\bar{O}\vec{v}_{cm_k/O})$ and flow velocity $(\bar{O}\vec{v}_{F/O})$. The flow velocity $(\bar{O}\vec{v}_{F/O})$ is defined in the IRF, and is translated into the body frames for each of the link to determine the flow velocity components in the body frames.

$$\begin{split} \Delta^{\bar{O}}\vec{v}_k &= [\Delta^{\bar{O}}\vec{v}_k, x]\vec{i}_{\bar{L}k} + [\Delta^{\bar{O}}\vec{v}_k, y]\vec{j}_{\bar{L}k} + [\Delta^{\bar{O}}\vec{v}_k, z]\vec{k}_{\bar{L}k} \\ \Delta^{\bar{O}}\vec{v}_k &= {}^{\bar{O}}\vec{v}_{cm_k/O} - {}^{\bar{L}_k}[C]^{\bar{O}}\{{}^{\bar{O}}\vec{v}_{F/O}\}_{\bar{O}} \end{split}$$

 $\Delta^{\vec{O}} \vec{v}_{k\perp}$ is the components of $\Delta^{\vec{O}} \vec{v}_k$ normal to the link or helical drive. For links (L_1, L_3, L_4, L_6) the directions normal to the link are in the \vec{i} and \vec{j} directions in the link body frame.

$$\Delta^{\bar{O}}\vec{v}_{k\perp} = [\Delta^{\bar{O}}\vec{v}_k,x]\vec{i}_{\bar{L}k} + [\Delta^{\bar{O}}\vec{v}_k,z]\vec{k}_{\bar{L}k}$$

For the helical drives (L_2, L_5) the directions normal to the link are in the \vec{j} and \vec{k} directions in the link body frame.

$$\Delta^{\bar{O}}\vec{v}_{k\perp} = [\Delta^{\bar{O}}\vec{v}_k,x]\vec{j}_{\bar{L}k} + [\Delta^{\bar{O}}\vec{v}_k,z]\vec{k}_{\bar{L}k}$$

 C_D is the drag coefficient calculated by

$$C_D = C_{D,basic} sin^2 \sigma_k \tag{28}$$

Where $C_{D,basic}$ is a constant based on the geometry, $C_{D,basic} = 1.1$ for a cylinder [6]. σ_k is the angle between the link or helical drive longitudinal axis and flow velocity. The σ_k for the links (L_1, L_3, L_4, L_6) , with longitudinal axis about \hat{j}_{L_k} , is

$$\sigma_k = \cos^{-1} \left(\frac{\bar{O}_{VF/O}}{|\bar{O}_{VF/O}|} \cdot \hat{j}_{\bar{L}_k} \right)$$

The σ_k for the helical drives (L_2, L_5) , with longitudinal axis about $\hat{i}_{\bar{L}_k}$, is

$$\sigma_k = \cos^{-1} \left(\frac{\vec{O}_{\vec{V}F/O}}{|\vec{O}_{\vec{V}F/O}|} \cdot \hat{i}_{\vec{L}_k} \right)$$

The flow acceleration force acting on the links and helical drives from the flow acceleration is proportional to the fluid that the links and helical drives displaced [6].

$$\vec{F}_{k,FA} = \rho V_k {}^{\bar{O}} \vec{a}_{F/O} \tag{29}$$

Where $\bar{O}\vec{a}_{F/O}$ is the acceleration of the flow.

$$\bar{O}\vec{a}_{F/O} = \bar{O}\frac{d}{dt}\bar{O}\vec{v}_{F/O}$$

3.6.2 Calculating Point Mass Forces. The forces acting on the point masses are approximated as point forces acting on a particle. The forces include gravity force $(\vec{F}_{m_p,grav})$. Assuming a frictionless system $(\vec{F}_{m_l,friction})$ is ignored. The forces acting on the x-direction point mass are

$$\vec{F}_{m_{p,x}} = \vec{F}_{m_{p,x},grav} \tag{30}$$

The forces acting on the y-direction point mass are

$$\vec{F}_{m_{p,y}} = \vec{F}_{m_{p,y},grav} \tag{31}$$

The gravity forces acting on the point masses are

$$\vec{F}_{m_{p,x},grav} = m_{p,x}(-g)\vec{k}_{\bar{o}} \tag{32}$$

$$\vec{F}_{m_{p,y},grav} = m_{p,y}(-g)\vec{k}_{\bar{o}} \tag{33}$$

3.6.3 Calculating Rover Forces. The forces acting on the rover are approximated as point forces acting at the center of mass. The forces include gravity force $(\vec{F}_{rov,grav})$, buoyancy force $(\vec{F}_{rov,B})$, drag force $(\vec{F}_{rov,drag})$, and flow acceleration force $(\vec{F}_{rov,FA})$. There are also reaction forces at each of the hinges and sliding mass positions $(\vec{F}_{rov,reaction})$. Assuming a frictionless system $(\vec{F}_{rov,friction})$ is ignored. Also assuming that the vehicle is slow moving, lift $(\vec{F}_{rov,lift})$ is ignored. The forces acting on the rover body are

$$\vec{F}_{rov} = \vec{F}_{rov,grav} + \vec{F}_{rov,B} + \vec{F}_{rov,drag} + \vec{F}_{rov,FA} + \vec{F}_{rov,reaction}$$
(34)

The gravity force acting on the rover in the inertial reference frame is

$$\vec{F}_{rov,grav} = m_{rov}(-g)\vec{k}_{\bar{o}} \tag{35}$$

The buoyancy force acting on the rover body chassis is proportional with the fluid that the rover body chassis displaces acting through the center of buoyancy for the rigid body [6]. The center of buoyancy is assumed to be equal to the center of mass due to the symmetry of the rigid bodies present in the system. The buoyancy force acting on the rover body chassis in the inertial reference frame, opposing the gravity force, is [6]

$$\vec{F}_{rov,B} = -\rho V_{rov}(-g)\vec{k}_{\bar{o}} \tag{36}$$

Where ρ is the density of the water and V_k is the volume of the fluid displaced by body k, which is approximated as the volume of the rover body.

$$V_{rov} = \frac{4}{3}\pi a^2 b$$

The drag acting on the rover body, assuming the rover is an ellipsoid with semi-major axis length b and semi-minor axis length a is broken into normal and axial components [8].

$$F_{rov,drag} = F_A \vec{i}_{\bar{R}} + F_{N_v} \vec{j}_{\bar{R}} + F_{N_z} \vec{k}_{\bar{R}}$$
 (37)

The axial force component, F_A acts about the center of mass in the $\vec{i}_{\vec{R}}$ direction of the rover body.

$$F_A = -\frac{1}{2}\rho C_{A_o} |\Delta^{\bar{O}}\vec{v}_{rov}|^2 (\Delta^{\bar{O}}\vec{v}_{rov} \cdot \vec{t}_{\bar{R}}) S_r$$
 (38)

The normal force component, F_N acts about the center of mass in the $\vec{j}_{\bar{R}}$ and $\vec{k}_{\bar{R}}$ direction of the rover body.

$$F_{N_y} = -\frac{1}{2}\rho C_{d_n} |\Delta^{\bar{O}} \vec{v}_{rov}|^2 (\Delta^{\bar{O}} \vec{v}_{rov} \cdot \vec{f}_{\bar{R}}) S_p$$
 (39)

$$F_{N_z} = -\frac{1}{2} \rho C_{d_n} |\Delta^{\bar{O}} \vec{v}_{rov}|^2 (\Delta^{\bar{O}} \vec{v}_{rov} \cdot \vec{k}_{\bar{R}}) S_p$$
 (40)

 C_{A_o} is the axial drag coefficient at zero angle of attack and α is the angle of attack [8]. For an ellipsoid $C_{A_o} = 0.25$ [9]. C_{d_n} is the cross-flow drag coefficient and α is the angle of attack [8]. For an ellipsoid $C_{d_n} \approx 1.2$ for Reynolds Number below 3×10^5 [10]. S_r is the reference area and S_p is the planform area. The

reference area for a ellipsoid is $S_r = \pi a^2$. The planform area for an ellipsoid is $S_p = \pi ab$.

 $\Delta^{\bar{O}} \vec{v}_{rov}$ is the difference between the rover velocity $(\bar{^O} \vec{v}_{R/O})$ and flow velocity $(\bar{^O} \vec{v}_{F/O})$. The flow velocity $(\bar{^O} \vec{v}_{F/O})$ is defined in the IRF, and is translated into the body frames for the rover chassis body frame to determine the flow velocity components normal and axial to the rover chassis.

$$\begin{split} {}^{\bar{O}}\vec{v}_{F/O} = & {}^{\bar{O}} \; v_{xF/O} \vec{i}_{\bar{O}} + {}^{\bar{O}} \; v_{y_{F/O}} \vec{j}_{\bar{O}} + {}^{\bar{O}} \; v_{z_{F/O}} \vec{k}_{\bar{O}} \\ \\ \{ {}^{\bar{O}}\vec{v}_{F/O} \}_{\bar{R}} = {}^{\bar{R}} [C]^{\bar{O}} \{ {}^{\bar{O}}\vec{v}_{F/O} \}_{\bar{O}} \\ \\ {}^{\bar{O}}\vec{v}_{F/O,R} = \{ {}^{\bar{O}}\vec{v}_{F/O} \}_{\bar{R}} \end{split}$$

$${}^{\bar{O}}\vec{v}_{F/O,R} = {}^{\bar{O}} \; v_{x,RF/O}\vec{i}_{\bar{R}} + {}^{\bar{O}} \; v_{y,RF/O}\vec{j}_{\bar{R}} + {}^{\bar{O}} \; v_{z,RF/O}\vec{k}_{\bar{R}}$$

$$\Delta^{\bar{O}}\vec{v}_{rov} = [^{\bar{O}}v_{xR/O} - ^{\bar{O}}v_{x,RF/O}]\vec{i}_{\bar{R}} + [^{\bar{O}}v_{yR/O} - ^{\bar{O}}v_{y,RF/O}]\vec{j}_{\bar{R}} + [^{\bar{O}}v_{zR/O} - ^{\bar{O}}v_{z,RF/O}]\vec{k}_{\bar{R}}$$
(41)

The flow acceleration force acting on the rover body from the flow acceleration is proportional to the fluid that the rover body displaced [6].

$$\vec{F}_{rov,FA} = \rho V_{rov}{}^{\bar{O}} \vec{a}_{F/O} \tag{42}$$

Where ${}^{\bar{O}}\vec{a}_{F/O}$ is the acceleration of the flow.

$$^{\bar{O}}\vec{a}_{F/O} = \frac{d}{dt}{}^{\bar{O}}\vec{v}_{F/O}$$

3.7 Torques

The torques acting on the links, helical drives, and rover chassis are calculated from the forces acting on the object about the center of mass of each rigid body. The gravity force, buoyancy force, drag force, and flow acceleration force are approximated as point forces acting on the bodies center of mass, so they generate no torque about the center of mass. The reaction forces from the link and hinge connections are found to cancel out in the system's equations of motion.

3.8 Added Mass

The added mass of the pressure distribution on the links from the fluid surrounding the links and rover body [6]. The added mass of the rigid bodies results in an effective inertia and is included in the mass and moment of inertia terms located in the generalized inertia force equations, F_R^* . The added mass approximations for cylinders are modeled as [6]

$$m_{k,add} = \frac{\rho \pi r_k^2 l_k}{4} \tag{43}$$

Where $V_k = \pi r_k^2 l_k$ and ρ is the density of the water. The added mass of each link and helical drive is calculated as

$$M_k = m_{k,add} + m_k = m_k + \frac{\rho \pi r_k^2 l_k}{4}$$
 (44)

The added mass term is applied to the normal components of the links and helical drives [6]. The added mass matrix for each link (L_1, L_3, L_4, L_6) is

$$\begin{split} \tilde{M}_{k} &= \left[m_{k} + \frac{\rho \pi r_{k}^{2} l_{k}}{4} \right] \vec{i}_{\bar{L}_{k}} \vec{i}_{\bar{L}_{k}} + \left[m_{k} \right] \vec{j}_{\bar{L}_{k}} \vec{j}_{\bar{L}_{k}} \\ &+ \left[m_{k} + \frac{\rho \pi r_{k}^{2} l_{k}}{4} \right] \vec{k}_{\bar{L}_{k}} \vec{k}_{\bar{L}_{k}} \end{split} \tag{45}$$

The added mass matrix for each helical drive (L_2, L_5) is

$$\tilde{M}_{k} = [m_{k}] \vec{i}_{\bar{L}_{k}} \vec{i}_{\bar{L}_{k}} + [m_{k} + \frac{\rho \pi r_{k}^{2} l_{k}}{4}] \vec{j}_{\bar{L}_{k}} \vec{j}_{\bar{L}_{k}}
+ [m_{k} + \frac{\rho \pi r_{k}^{2} l_{k}}{4}] \vec{k}_{\bar{L}_{k}} \vec{k}_{\bar{L}_{k}} \quad (46)$$

The total mass moment of inertia terms for each link (L_1, L_3, L_4, L_6) about each link center of mass, approximated as a thin rod, is

$$\tilde{I}_{cm_k,tot} = \left[\frac{1}{12} M_k l_k^2 \right] \vec{i}_{\bar{L}_k} \vec{i}_{\bar{L}_k} + [0] \, \vec{j}_{\bar{L}_k} \vec{j}_{\bar{L}_k} + \left[\frac{1}{12} M_k l_k^2 \right] \vec{k}_{\bar{L}_k} \vec{k}_{\bar{L}_k}$$

The total mass moment of inertia for each helical drive (L_2, L_5) about each helical drive center of mass, approximated currently as a thin rod, is

$$\tilde{I}_{cm_k,tot} = [0] \vec{i}_{\bar{L}_k} \vec{i}_{\bar{L}_k} + \left[\frac{1}{12} M_k l_k^2 \right] \vec{j}_{\bar{L}_k} \vec{j}_{\bar{L}_k} + \left[\frac{1}{12} M_k l_k^2 \right] \vec{k}_{\bar{L}_k} \vec{k}_{\bar{L}_k}$$

The added mass for the rover chassis, modeled as an ellipsoid, is approximated using the added mass equation [11].

$$m_{rov,add} = \rho V_{rov} c_m \tag{47}$$

Where c_m is the added mass, or hydrodynamic mass, coefficient for a given geometry. The added mass coefficient for an ellipsoid is broken into components of vertical motion, c_{m_y} and c_{m_z} , and horizontal motion, c_{m_x} .

$$\begin{split} \tilde{M}_{rov} &= [m_{rov} + \rho V_{rov} c_{m_x}] \vec{i}_{\vec{R}} \vec{i}_{\vec{R}} + [m_{rov} + \rho V_{rov} c_{m_y}] \vec{j}_{\vec{R}} \vec{j}_{\vec{R}} \\ &+ [m_{rov} + \rho V_{rov} c_{m_z}] \vec{k}_{\vec{R}} \vec{k}_{\vec{R}} \end{split} \tag{48}$$

When b/a = 2 is approximated to be $c_{m_x} = 0.225$ and $c_{m_y} = c_{m_z} = 0.7$ [11]. The added mass moment of inertia for an ellipsoid about the minor axis can be calculated using

$$\tilde{I}_{R,add} = [0] \vec{i}_{\bar{R}} \vec{i}_{\bar{R}} + \left[\frac{1}{5} \rho V_{rov} c_I(a^2 + b^2) \right] \vec{j}_{\bar{R}} \vec{j}_{\bar{R}} + \left[\frac{1}{5} \rho V_{rov} c_I(a^2 + b^2) \right] \vec{k}_{\bar{R}} \vec{k}_{\bar{R}} \tag{49}$$

The added mass moment of inertia coefficient, c_I , about the minor axis when b/a = 2 is approximated to be $c_{I_y} = c_{I_z} = 0.225$ [11]. There is no added mass moment of inertia about the ellipsoid major axis. Therefore the total moment of inertia tensor for the rover is

$$\begin{split} \tilde{I}_{R,tot} &= [\frac{1}{5} m_{rov} (a^2 + a^2)] \vec{i}_{R} \vec{i}_{\bar{R}} + [\frac{1}{5} (m_{rov} + \rho V_{rov} c_I) (a^2 \\ &+ b^2)] \vec{j}_{\bar{R}} \vec{j}_{\bar{R}} + [\frac{1}{5} (m_{rov} + \rho V_{rov} c_I) (a^2 + b^2)] \vec{k}_{\bar{R}} \vec{k}_{\bar{R}} \end{split} \tag{50}$$

The added mass and added mass moment of inertia terms are incorporated into the general inertia force equation.

$$F_{r}^{*} = -\sum_{k=1}^{N_{R}} (\tilde{M}_{k} \cdot \bar{\sigma} \vec{a}_{cm_{k}/O} \cdot \bar{\sigma} \vec{v}_{cm_{k},r} + ((\tilde{I}_{cm_{k},tot} \cdot \bar{O} \vec{\alpha}^{\bar{B}_{k}} + \bar{O} \vec{\alpha}^{\bar{B}_{k}})) \cdot \bar{O} \vec{\omega}_{r}^{\bar{B}_{k}}) - \sum_{l=1}^{N_{P}} m_{l} \bar{\sigma} \vec{a}_{m_{l}/O} \cdot \bar{O} \vec{v}_{m_{l},r}$$

$$(51)$$

4. NUMERICAL SIMULATION

All of these equations can be substitute into $F_r + F_r^* = 0$ for each generalize motion to calculate the equations of motion. Making the following geometric assumptions of the system

$$\begin{aligned} d_1 &= d_3 = d_4 = d_6 = 0.5 in = 0.0127 m \\ l_1 &= l_3 = l_4 = l_6 = 10 in = 0.254 m \\ d_2 &= d_5 = 2.5 in = 0.0635 m \\ l_2 &= l_5 = 12.5 in = 0.3175 m \\ 2b &= \frac{d_1}{2} + l_2 + \frac{d_3}{2} \\ a &= b/2 \\ g &= 9.81 m/s \\ \rho &= 998.2 \frac{kg}{m^3} \end{aligned}$$

The following specific case was applied to calculate the equations of motion. The helical drives are out to the side in line with the center of mass of the rover chassis body and are modeled as constants.

$$\begin{array}{l} \theta_A = \theta_B = \frac{\pi}{2} \\ \theta_C = \theta_D = \frac{\pi}{2} \\ \dot{\theta}_A = \dot{\theta}_B = 0 \\ \dot{\theta}_C = \dot{\theta}_D = 0 \\ \ddot{\theta}_A = \ddot{\theta}_B = 0 \\ \ddot{\theta}_C = \ddot{\theta}_D = 0 \end{array}$$

The natural buoyancy of the system and the gravity of the system are calculated to make the forces cancel out, $\vec{F}_{k,grav} + \vec{F}_{k,B} = 0$. The required masses of each link, given the dimensions stated, to cancel out the gravity and natural buoyancy of the rigid bodies can be calculated from

$$\begin{split} \vec{F}_{k,grav} &= -\vec{F}_{k,B} \\ m_k(-g) &= -(-\rho V_k(-g)) \\ m_k &= \rho V_k = \rho \pi \frac{d_k}{2} l_k \end{split}$$

The helical drive masses are $m_2 = m_5 \approx 1kg$. The link masses are $m_1 = m_3 = m_4 = m_6 \approx 0.32kg$. The required masses of the rover chassis, given the dimensions stated, to calculate the total mass required to cancel out the natural buoyancy of the rover chassis

$$\begin{split} \vec{F}_{rov,grav} &= -\vec{F}_{rov,B} \\ m_{rov}(-g) &= -(-\rho V_{rov}(-g)) \\ m_{rov} &= \rho V_k = \rho \frac{4}{3}\pi a^2 b \end{split}$$

The total mass of the rover chassis and the sliding masses is $m_{rov} \approx 4.70 kg$. The only buoyancy from the system comes from the ballast system filling or draining $(\vec{F}_{k,buoynet})$. For cases where

the sliding masses are present the mass of the sliding masses is selected to be $m_{p,x}=m_{p,y}=0.5kg$. The added mass from the sliding masses will be offset by $\vec{F}_{k,buoynet}$ to prevent sinking. The water in this case is assumed to be static, and therefore has no flow velocity or acceleration.

$$\vec{O}\vec{v}_{F/O} = 0\vec{i}_{\bar{O}} + 0\vec{j}_{\bar{O}} + 0\vec{k}_{\bar{O}}$$

. The differential equations of motion were simulated in MAT-LAB using ode45(), at initial values $q_1(0) = q_2(0) = q_3(0) = q_4(0) = q_5(0) = q_6(0) = \dot{q}_1(0) = \dot{q}_2(0) = \dot{q}_3(0) = \dot{q}_4(0) = \dot{q}_5(0) = \dot{q}_6(0) = 0$.

5. RESULTS

The dynamic model was simulated for various cases to demonstrate the rover's underwater capabilities.

5.1 Forward Thrust

The net thrust from the helical drives provides a forward motion. In the case the net thrust and net buoyancy forces were set to be

$$\vec{F}_{2,thrustnet} = 10N$$

$$\vec{F}_{5,thrustnet} = 10N$$

$$\vec{F}_{2,buoynet} = \frac{m_{p,x}g}{2} + \frac{m_{p,y}g}{2}N$$

$$\vec{F}_{5,buoynet} = \frac{m_{p,x}g}{2} + \frac{m_{p,y}g}{2}N$$

The net buoyancy accounts for the weight of the sliding masses, split evenly between the two helical drives. This prevents the rover from sinking due to the additional mass from the sliding masses and allows a distinct demonstration of how the rover will perform when the sliding masses are off center.

The location of the sliding masses for this case are located at the center of mass of the rover body.

$$x_p = 0\vec{i}_{\bar{R}}$$
$$y_p = 0\vec{j}_{\bar{R}}$$

The overall path of the rover in the $x_{\bar{O}}$, $y_{\bar{O}}$, and $z_{\bar{O}}$ directions is plotted in Fig. 4. The rover experiences a brief acceleration when it first begins moving from rest, and then the position increases linearly and the rover velocity is constant. This provides a base case for the rover in a forward motion, to confirm the expected motion when both helical drives have the same amount of net thrust.

5.2 Rise from Buoyancy

The net buoyancy from the helical drives provides a rising motion. In the case the net thrust and net buoyancy forces were set to be

$$\begin{split} \vec{F}_{2,thrustnet} &= 0N \\ \vec{F}_{5,thrustnet} &= 0N \\ \vec{F}_{2,buoynet} &= \frac{m_{p,x}g}{2} + \frac{m_{p,y}g}{2} + 10N \\ \vec{F}_{5,buoynet} &= \frac{m_{p,x}g}{2} + \frac{m_{p,y}g}{2} + 10N \end{split}$$

The net buoyancy accounts for the weight of the sliding masses, split evenly between the two helical drives. This prevents the rover from sinking due to the additional mass from the sliding

masses and allows a distinct demonstration of how the rover will perform when the sliding masses are off center.

The location of the sliding masses for this case are located at the center of mass of the rover body.

$$x_p = 0\vec{i}_{\bar{R}}$$
$$y_p = 0\vec{j}_{\bar{R}}$$

The overall path of the rover in the $x_{\bar{O}}$, $y_{\bar{O}}$, and $z_{\bar{O}}$ directions is plotted in Fig. 5. The rover experiences a brief acceleration when it first begins moving from rest, and then the position increases linearly and the rover velocity is constant. This provides a base case for the rover in a rising motion, to confirm the expected motion when both helical drives have the same amount of net buoyancy.

5.3 Yaw from Thrust Variation

The net thrust from the helical drives provides a forward motion, and when the forces are not equal will result in the rover yawing. The rover the net thrust and net buoyancy forces were set to be

$$\begin{aligned} \vec{F}_{2,thrustnet} &= 10N \\ \vec{F}_{5,thrustnet} &= 5N \\ \vec{F}_{2,buoynet} &= \frac{m_{p,x}g}{2} + \frac{m_{p,y}g}{2}N \\ \vec{F}_{5,buoynet} &= \frac{m_{p,x}g}{2} + \frac{m_{p,y}g}{2}N \end{aligned}$$

The net buoyancy accounts for the weight of the sliding masses, split evenly between the two helical drives. This prevents the rover from sinking due to the additional mass from the sliding masses and allows a distinct demonstration of how the rover will perform when the sliding masses are off center.

The location of the sliding masses for this case are located at the center of mass of the rover body.

$$x_p = 0\vec{i}_{\bar{R}}$$
$$y_p = 0\vec{j}_{\bar{R}}$$

A top view of the rover path in the x-y plane in Fig. 6 shows the path of the rover in the $x_{\bar{O}}$ and $y_{\bar{O}}$ directions. The yaw, ψ , position of the rover vs time is plotted in Fig. 6. The rover experiences an angular acceleration when it first begins moving from rest, and then the angular velocity approaches constant and the rover reaches a constant diameter circular path in congruent circles as confirmed in the x position of the rover vs time plot in Fig. 6.

5.4 Roll Motion

The rover has two methods of implementing roll, the net buoyancy and the y-direction sliding mass.

5.4.1 Roll from Buoyancy in Helical Drive. The net buoyancy from the helical drives provides a rising motion, and when the forces are not equal will result in the rover rolling. The rover the net thrust and net buoyancy forces were set to be

$$\vec{F}_{2,thrustnet} = 0N$$

$$\vec{F}_{5,thrustnet} = 0N$$

$$\vec{F}_{2,buoynet} = \frac{m_{p,x}g}{2} + \frac{m_{p,y}g}{2} + 10N$$

$$\vec{F}_{5,buoynet} = \frac{m_{p,x}g}{2} + \frac{m_{p,y}g}{2}N$$

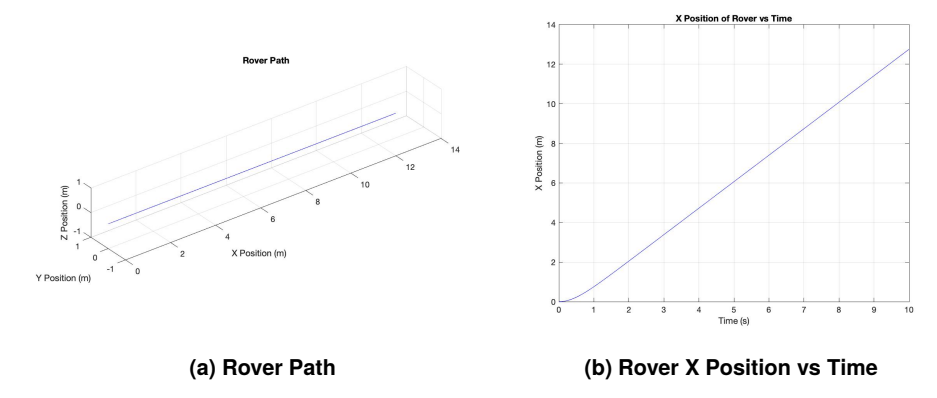


FIGURE 4: FORWARD MOTION FROM THRUST GENERALIZED COORDINATE PLOTS

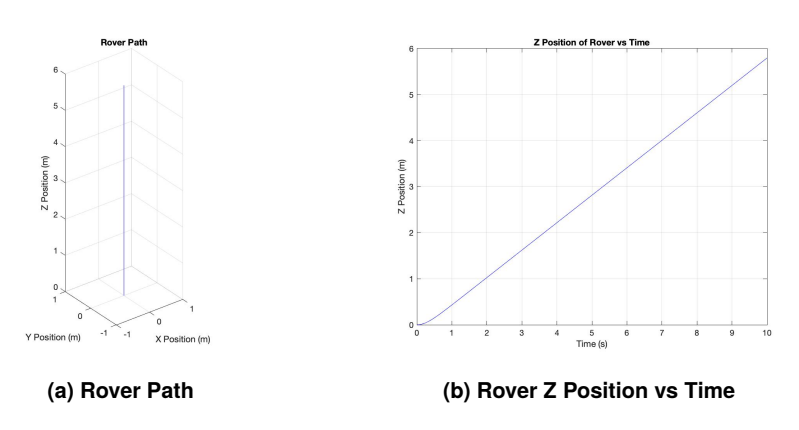


FIGURE 5: RISE FROM BUOYANCY GENERALIZED COORDINATE PLOTS

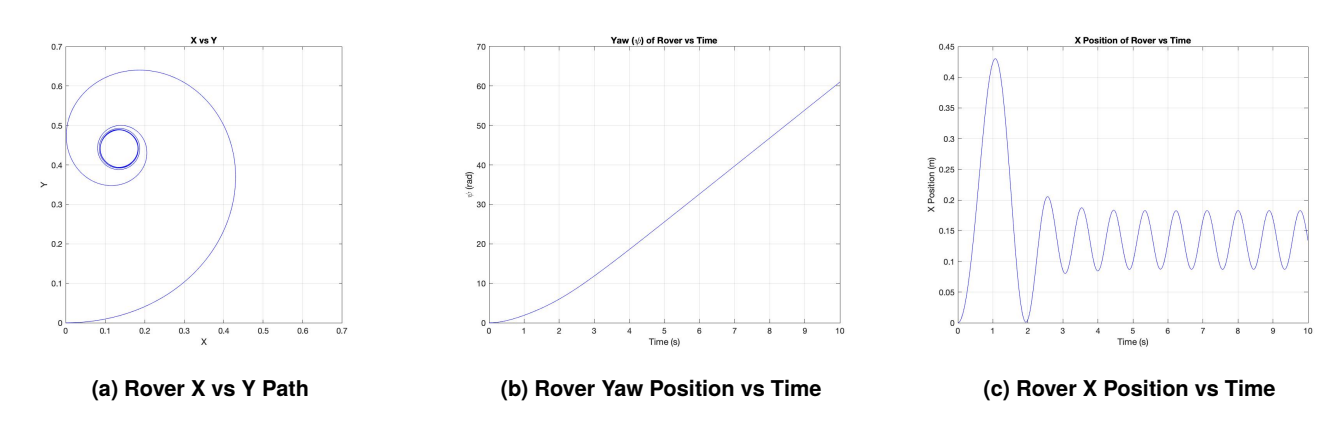


FIGURE 6: YAW FROM THRUST GENERALIZED COORDINATE PLOTS

The net buoyancy accounts for the weight of the sliding masses, split evenly between the two helical drives. This prevents the rover from sinking due to the additional mass from the sliding masses and allows a distinct demonstration of how the rover will perform when the sliding masses are off center.

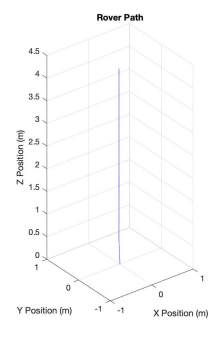
The location of the sliding masses for this case are located at the center of mass of the rover body.

$$x_p = 0\vec{i}_{\bar{R}}$$
$$y_p = 0\vec{j}_{\bar{R}}$$

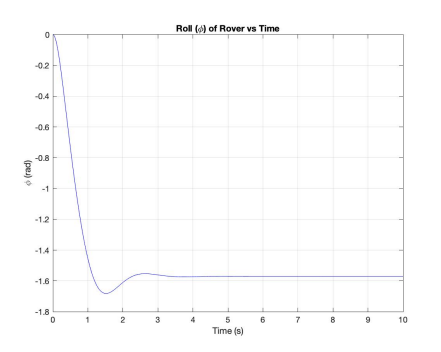
The overall path of the rover in the $x_{\bar{O}}$, $y_{\bar{O}}$, and $z_{\bar{O}}$ directions is plotted in Fig. 7. The roll, ϕ , position of the rover vs time is

plotted in Fig. 7. The rover experiences an angular acceleration when it first begins moving from rest, and then the roll rotation overshoots $\frac{\pi}{2}$ and then returns and levels out at $\frac{\pi}{2}$, where the rover is now balanced on its side. As the rover rotates from net buoyancy, the rover experiences roll motion, as well as motion in the $z_{\bar{O}}$ direction from the continuous positive net buoyancy.

5.4.2 Roll from Sliding Mass Moment. The y-direction sliding mass moving away from the center of mass of the rover chassis, will apply a moment about the rover center of mass in the rolling direction. The rover the net thrust and net buoyancy forces were set to be







(b) Rover Roll Position vs Time

FIGURE 7: ROLL FROM BUOYANCY GENERALIZED COORDINATE PLOTS

$$\vec{F}_{2,thrustnet} = 0N$$

$$\vec{F}_{5,thrustnet} = 0N$$

$$\vec{F}_{2,buoynet} = \frac{m_{p,x}g}{2} + \frac{m_{p,y}g}{2}N$$

$$\vec{F}_{5,buoynet} = \frac{m_{p,x}g}{2} + \frac{m_{p,y}g}{2}N$$

There is no motion from the net thrust and net buoyancy applied in this case. The net buoyancy accounts for the weight of the sliding masses, split evenly between the two helical drives. This prevents the rover from sinking due to the additional mass from the sliding masses and allows a distinct demonstration of how the rover will perform when the sliding masses are off center. The location of the x-direction sliding mass is located at the center of mass of the rover body and the y-direction sliding mass is located 3 inches from center of mass of the rover body in the $\vec{j}_{\vec{R}}$ direction.

$$\begin{aligned} x_p &= 0 \vec{i}_{\bar{R}} \\ y_p &= \left[3in \right] \vec{j}_{\bar{R}} = \left[0.0762m \right] \vec{j}_{\bar{R}} \end{aligned}$$

The overall path of the rover in the $x_{\bar{O}}$, $y_{\bar{O}}$, and $z_{\bar{O}}$ directions is plotted in Fig. 8. As the rover rotates from the y-direction sliding mass, the rover experiences roll motion as well as movement in the $y_{\bar{O}}$ and $z_{\bar{O}}$ direction as the rover adjusts to the new y_p location. The roll, ϕ , position of the rover of the rover vs time is plotted in Fig. 8. The rover experiences an angular acceleration, the magnitude of the roll rotation overshoots $\frac{\pi}{2}$ and then returns and oscillates about $\frac{\pi}{2}$, where the rover is now on its side. The roll from the y-direction sliding mass is oscillatory, while the roll from the net buoyancy reaches a steady solution relatively quickly. However the roll from the y-direction sliding mass does not change the position of the rover as much as the roll from the net buoyancy.

5.5 Pitch from Sliding Mass Moment

The x-direction sliding mass moving away from the center of mass of the rover chassis, will apply a moment about the rover center of mass in the pitching direction. The rover the net thrust and net buoyancy forces were set to be

$$\begin{aligned} \vec{F}_{2,thrustnet} &= 10N \\ \vec{F}_{5,thrustnet} &= 10N \\ \vec{F}_{2,buoynet} &= \frac{m_{p,x}g}{2} + \frac{m_{p,y}g}{2}N \\ \vec{F}_{5,buoynet} &= \frac{m_{p,x}g}{2} + \frac{m_{p,y}g}{2}N \end{aligned}$$

There is a forward motion from the net thrust applied in this case. The net buoyancy accounts for the weight of the sliding masses, split evenly between the two helical drives. This prevents the rover from sinking due to the additional mass from the sliding masses and allows a distinct demonstration of how the rover will perform when the sliding masses are off center.

The location of the y-direction sliding mass is located at the center of mass of the rover body and the x-direction sliding mass is located 3 inches from center of mass of the rover body in the $-\vec{i}_{R}$ direction.

$$x_{p} = [-3in]\vec{i}_{\vec{R}} = [-0.0762m]\vec{i}_{\vec{R}}$$

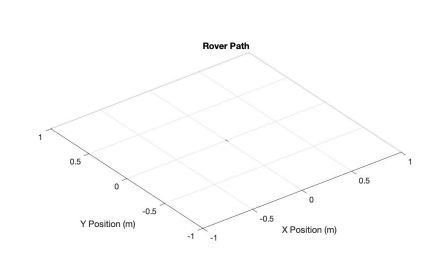
$$y_{p} = 0\vec{j}_{\vec{R}}$$

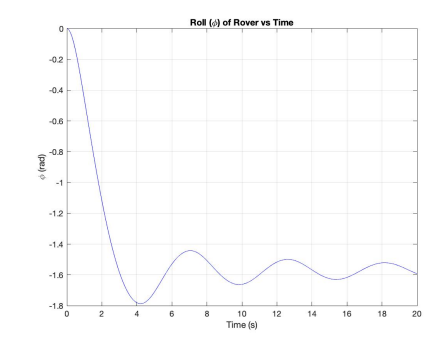
The overall path of the rover in the $x_{\bar{O}}$, $y_{\bar{O}}$, and $z_{\bar{O}}$ directions is plotted in Fig. 9. As the rover pitches upward from the x-direction sliding mass, the rover experiences pitch motion as well as upward movement in the $z_{\bar{O}}$ direction as the rover continues to propel forward from net thrust in the $i_{\bar{R}}$ direction.

The pitch, θ , position of the rover vs time is plotted in Fig. 9. The rover experiences an angular acceleration, the pitch rotation approaches $\frac{\pi}{2}$, where the rover is now facing the $\vec{k}_{\bar{O}}$ direction.

6. CONCLUSION

Kane's method successfully models the underwater motion for the MAARCO rover. The model includes the expected hydrodynamic forces acting on the rover, as well as other generated forces from the system such as net thrust, net buoyancy, and control forces. The model confirms that the rover motion can be controlled by the helical drive thrust, helical drive ballast system buoyancy, and the position of the sliding masses by inducing a linear or angular acceleration on the rover body system. The model has the ability to model transient effects of a hydrodynamic environment. The thrust from the helical drives will produce a forward acceleration, and the imbalance of thrust is confirmed to result in a yaw angular acceleration about the rover chassis center. The buoyancy from the helical drives will produce a upward acceleration, and the imbalance of buoyancy is confirmed to result in a roll angular acceleration about the rover chassis center. The x-direction sliding mass gravity force offset from the center of the rover chassis will produce a moment about the y-axis, that results in a pitch angular acceleration about the rover chassis center. The

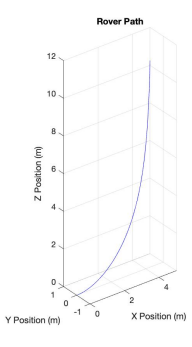




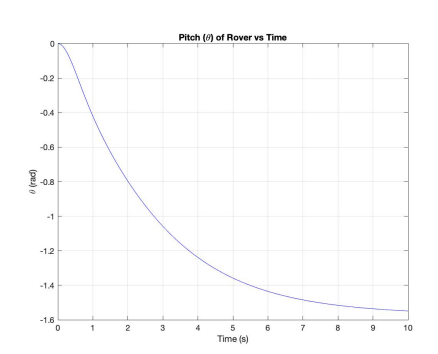
(a) Rover Path

(b) Rover Roll Position vs Time

FIGURE 8: ROLL FROM SLIDING MASS WITH NO MOTION GENERALIZED COORDINATE PLOTS



(a) Rover Path



(b) Rover Pitch Position vs Time

FIGURE 9: PITCH UP FROM SLIDING MASS WITH FORWARD MOTION GENERALIZED COORDINATE PLOTS

y-direction sliding mass gravity force offset from the center of the rover chassis will produce a moment about the x-axis, that results in a roll angular acceleration about the rover chassis center. These base cases behave as expected from the applied motion to the rover system, and demonstrate the success of Kane's method modeling.

This method provided a simplified model for a complex system, with lower computational cost, and the ability to numerically simulate the rover motion underwater. This dynamic model demonstrates the capabilities of the rover underwater and provides a model to further develop controls methods for specific cases and missions as the resulting linear and angular positions are calculated. Specific control equations can be applied to the sliding masses position and motion, the thrust of the helical drives, and the buoyancy of the helical drive ballast to control the system performance based on the design and desired mission requirements. Future work for a more complete model would include investigation into more accurate helical drive properties, including the net thrust force, net buoyancy force, moment of inertia from further helical drive design and studies. These additional studies could be implemented in the dynamic model equations described above for a more accurate model. Different cases would also provide additional insight on the behavior of the underwater vehicle.

ACKNOWLEDGMENTS

The authors would like to acknowledge funding for this research provided by the National Science Foundation under award

no. cmMI-2116216, which is managed by Dr. Alex Leonessa. The authors would also like to acknowledge support resources from North Carolina Stat University, as well as support and assistance from the MAARCO team.

REFERENCES

- [1] "MAARCO: Multi-terrain Amphibious ARCtic ExplOrer." National Science Foundation (2021). URL https://www.nsf.gov/awardsearch/showAward?AWD_ID= 2116216&HistoricalAwards=false.
- [2] Lynch, Ryan, Beknalkar, Sumedh, Bishop, Riley, Crow, Arin, Donohue, Brigid, Pacheco-Cay, Cristian, Smith, Alaina, Mazzoleni, Andre and Bryant, Matthew. "Design and Construction of a Terrestrial Testing Rig for Experimentation and Analysis of Multi-Terrain Screw-Propelled Vehicle Dynamics and Performance." (In Press).
- [3] Beknalkar, Sumedh, Varanwa, Aditya, Lynch, Ryan, Bryant, Matthew and Mazzoleni, Andre. "Modeling and Analysis of Terrestrial Locomotion Dynamics of Helical Drive-Propelled Multi-Terrain." (In Press).
- [4] Donohue, Brigid, Beknalkar, Sumedh, Bryant, Matthew and Mazzoleni, Andre. "Modeling Underwater Propulsion of a Helical Drive Using Computational Fluid Dynamics for an Amphibious Rover." (In Press).
- [5] Vadlamannati, Ashwin, Beknalkar, Sumedh, Best, Dustin, Bryant, Matthew and Mazzoleni, Andre. "Design, Proto-

- typing and Experiments Using Small-Scale Helical Drive Rover for Multi-Terrain Exploration." (In Press).
- [6] Tarn, T.J., Shoults, G.A. and S.P.Yang. "A Dynamic Model of an Underwater Vehicle with a Robotic Manipulator using Kane's Method." *Autonomous Robots 3* (1996).
- [7] Kane, Thomas R. and Levinson, David A. *Dynamics Theory and Applications*. McGraw-Hill (1985).
- [8] MacLeod, Marc and Bryant, Matthew. "Dynamic Modeling, Analysis, and Testing of a Variable Buoyancy System for Unmanned Multidomain Vehicles." *IEEE Journal of Oceanic Engineering* Vol. 42 No. 3 (2017).
- [9] Cengel, Y. and Cimbala, J. Fluid Mechanics: Fundamentals and Applications, 2nd ed. McGraw-Hill, New York, NY, USA (2010).
- [10] Jorgensen, L. "Prediction of static aerodynamic characteristics for space- shuttle-like and other bodies at angles of attack from 0 to 180." NASA TN D-6996 (1973).
- [11] Chung, H. and Chen, S.S. "Hydrodynamic Mass." *ASME* pressure vessel and piping conference (1984).

APPENDIX A. DIRECTION COSINE MATRICES ROVER SYSTEM

For side A-B, the direction cosine matrices between \bar{A} and \bar{R} as well as \bar{B} and \bar{R} are

$${}^{\bar{A}}[C]^{\bar{R}} = {}^{\bar{B}}[C]^{\bar{R}} = \begin{bmatrix} 1 & 0 & 0 \\ 0 & \cos\frac{\pi}{2} & \sin\frac{\pi}{2} \\ 0 & -\sin\frac{\pi}{2} & \cos\frac{\pi}{2} \end{bmatrix}$$

The direction cosine matrices for the A-B side link and helical drive body frames are

$$\bar{L}_{1}[C]^{\bar{A}} = \begin{bmatrix} 1 & 0 & 0 \\ 0 & cos\theta_{A} & sin\theta_{A} \\ 0 & -sin\theta_{A} & cos\theta_{A} \end{bmatrix}$$

$$\bar{L}_2[C]^{\bar{L}_1} = \begin{bmatrix} 1 & 0 & 0 \\ 0 & 1 & 0 \\ 0 & 0 & 1 \end{bmatrix}$$

$$\bar{L}_3[C]^{\bar{L}_2} = \begin{bmatrix} 1 & 0 & 0 \\ 0 & 1 & 0 \\ 0 & 0 & 1 \end{bmatrix}$$

$$\bar{L_3}[C]^{\bar{B}} = \begin{bmatrix} 1 & 0 & 0 \\ 0 & \cos\theta_B & \sin\theta_B \\ 0 & -\sin\theta_B & \cos\theta_B \end{bmatrix} = \begin{bmatrix} 1 & 0 & 0 \\ 0 & \cos\theta_A & \sin\theta_A \\ 0 & -\sin\theta_A & \cos\theta_A \end{bmatrix}$$

For side C-D, the direction cosine matrices between \bar{C} and \bar{R} as well as \bar{D} and \bar{R} are

$$\bar{C}[C]^{\bar{R}} = \bar{D}[C]^{\bar{R}} \begin{bmatrix} 1 & 0 & 0 \\ 0 & \cos\frac{\pi}{2} & \sin\frac{\pi}{2} \\ 0 & -\sin\frac{\pi}{2} & \cos\frac{\pi}{2} \end{bmatrix} \begin{bmatrix} \cos\pi & \sin\pi & 0 \\ -\sin\pi & \cos\pi & 0 \\ 0 & 0 & 1 \end{bmatrix}$$

The direction cosine matrices for the C-D side link and helical drive body frames are

$$\bar{L}_{4}[C]^{\bar{C}} = \begin{bmatrix} 1 & 0 & 0 \\ 0 & \cos\theta_{C} & \sin\theta_{C} \\ 0 & -\sin\theta_{C} & \cos\theta_{C} \end{bmatrix}$$

$$\bar{L}_{4}[C]^{\bar{L}_{5}} = \begin{bmatrix} 1 & 0 & 0 \\ 0 & 1 & 0 \\ 0 & 0 & 1 \end{bmatrix}$$

$$\bar{L}_{5}[C]^{\bar{L}_{6}} = \begin{bmatrix} 1 & 0 & 0 \\ 0 & 1 & 0 \\ 0 & 0 & 1 \end{bmatrix}$$

$$\bar{L_6}[C]^{\bar{D}} = \begin{bmatrix} 1 & 0 & 0 \\ 0 & \cos\theta_D & \sin\theta_D \\ 0 & -\sin\theta_D & \cos\theta_D \end{bmatrix} = \begin{bmatrix} 1 & 0 & 0 \\ 0 & \cos\theta_C & \sin\theta_C \\ 0 & -\sin\theta_C & \cos\theta_C \end{bmatrix}$$

APPENDIX B. POSITION VECTORS ROVER SYSTEM

The position vectors of the hinges of the system from the rover chassis center of mass are

$$\begin{split} \vec{r}_{A/R} &= -b\vec{i}_{\bar{R}} + 0\vec{j}_{\bar{R}} + 0\vec{k}_{\bar{R}} \\ \vec{r}_{B/R} &= b\vec{i}_{\bar{R}} + 0\vec{j}_{\bar{R}} + 0\vec{k}_{\bar{R}} \\ \vec{r}_{C/R} &= -b\vec{i}_{\bar{R}} + 0\vec{j}_{\bar{R}} + 0\vec{k}_{\bar{R}} \\ \vec{r}_{D/R} &= b\vec{i}_{\bar{R}} + 0\vec{j}_{\bar{R}} + 0\vec{k}_{\bar{R}} \end{split}$$

The position vectors for the links and helical drive on the A-B side are

$$\vec{r}_{L_1/A} = \vec{r}_{cm_1/A} = 0\vec{i}_{\bar{L}_1} - \frac{l_1}{2}\vec{j}_{\bar{L}_1} + 0\vec{k}_{\bar{L}_1}$$

$$\begin{split} \vec{r}_{L_2/L_1} &= \vec{r}_{cm_2/cm_1} = \left[\frac{d_1}{2} + \frac{l_2}{2}\right] \vec{i}_{\bar{L}_2} - \frac{l_1}{2} \vec{j}_{\bar{L}_2} + 0 \vec{k}_{\bar{L}_2} \\ \\ \vec{r}_{L_2'/L_1} &= 0 \vec{i}_{\bar{L}_2} + 0 \vec{j}_{\bar{L}_2} + 0 \vec{k}_{\bar{L}_2} \end{split}$$

$$\vec{r}_{L_3/L_2} = \vec{r}_{cm_3/cm_2} = \left[\frac{d_3}{2} + \frac{l_2}{2}\right] \vec{i}_{\bar{L}_3} + \frac{l_3}{2} \vec{j}_{\bar{L}_3} + 0 \vec{k}_{\bar{L}_3}$$

$$\vec{r}_{B/L_3} = \vec{r}_{B/cm_3} = 0\vec{i}_{\bar{L}_3} + \frac{l_3}{2}\vec{j}_{\bar{L}_3} + 0\vec{k}_{\bar{L}_3}$$

The position vectors for the links and helical drive on the C-D side are

$$\vec{r}_{L_6/D} = \vec{r}_{cm_6/D} = 0\vec{i}_{\bar{L}_6} - \frac{l_6}{2}\vec{j}_{\bar{L}_6} + 0\vec{k}_{\bar{L}_6}$$

$$\vec{r}_{L_5/L_6} = \vec{r}_{cm_5/cm_6} = \left[\frac{d_6}{2} + \frac{l_5}{2}\right] \vec{i}_{\bar{L}_5} - \frac{l_6}{2} \vec{j}_{\bar{L}_5} + 0 \vec{k}_{\bar{L}_5}$$

$$\vec{r}_{L_5'/L_5} = 0 \vec{i}_{\bar{L}_5} + 0 \vec{j}_{\bar{L}_5} + 0 \vec{k}_{\bar{L}_5}$$

$$\vec{r}_{L_4/L_5} = \vec{r}_{cm_4/cm_5} = \left[\frac{d_4}{2} + \frac{l_5}{2}\right] \vec{i}_{\bar{L}_4} + \frac{l_4}{2} \vec{j}_{\bar{L}_4} + 0 \vec{k}_{\bar{L}_4}$$

$$\vec{r}_{C/L_4} = \vec{r}_{C/cm_4} = 0\vec{i}_{\bar{L}_4} + \frac{l_4}{2}\vec{j}_{\bar{L}_4} + 0\vec{k}_{\bar{L}_4}$$

The position vectors to relate the links and helical drives from the inertial reference frame can be calculated. The position vectors for side A-B are

$$\vec{r}_{A/O} = \vec{r}_{A/R} + \vec{r}_{R/O}$$

$$\vec{r}_{B/O} = \vec{r}_{B/R} + \vec{r}_{R/O}$$

$$\vec{r}_{L_1/O} = \vec{r}_{cm_1/O} = \vec{r}_{cm_1/A} + \vec{r}_{A/O}$$

$$\vec{r}_{L_2/O} = \vec{r}_{cm_2/O} = \vec{r}_{cm_2/cm_1} + \vec{r}_{cm_1/O}$$

$$\vec{r}_{L_3/O} = \vec{r}_{cm_3/O} = \vec{r}_{cm_3/cm_2} + \vec{r}_{cm_2/O}$$

The position vectors for side C-D are

$$\vec{r}_{C/O} = \vec{r}_{C/R} + \vec{r}_{R/O}$$

$$\vec{r}_{D/O} = \vec{r}_{D/R} + \vec{r}_{R/O}$$

$$\vec{r}_{L_6/O} = \vec{r}_{cm_6/O} = \vec{r}_{cm_6/D} + \vec{r}_{D/O}$$

$$\vec{r}_{L_5/O} = \vec{r}_{cm_5/O} = \vec{r}_{cm_5/cm_6} + \vec{r}_{cm_6/O}$$

$$\vec{r}_{L_4/O} = \vec{r}_{cm_4/O} = \vec{r}_{cm_4/cm_5} + \vec{r}_{cm_5/O}$$

Then the position vectors can be rotated back into the body frame using the direction cosine matrices. The position vectors can be used to calculate the velocity and acceleration for each of the links an helical drives.

$$\bar{O}_{\vec{v}_{cm_k/O}} = \bar{O}_{\vec{d}t} \vec{r}_{cm_k/O}$$

$$= \bar{L}_k \frac{d}{dt} \vec{r}_{cm_k/O} + \bar{O}_{\vec{b}} \omega^{\vec{L}_k} \times \vec{r}_{cm_k/O} \quad (52)$$

$$\bar{O}_{\vec{d}_{cm_k/O}} = \bar{O}_{\vec{d}} \frac{d}{dt} \bar{O}_{\vec{v}_{cm_k/O}}$$

$$= \bar{L}_k \frac{d}{dt} \bar{O}_{\vec{v}_{cm_k/O}} + \bar{O}_{\vec{v}_{cm_k/O}} \times \bar{O}_{\vec{v}_{cm_k/O}}$$
(53)

The angular velocities between the link and helical drive body frames and the inertial reference frame \bar{O}

$${}^{\bar{O}}\vec{\omega}^{\bar{L}_k} = {}^{\bar{O}}\omega_x{}^{\bar{L}_k}\vec{i}_{\bar{L}_k} + {}^{\bar{O}}\omega_y{}^{\bar{L}_k}\vec{j}_{\bar{L}_k} + {}^{\bar{O}}\omega_z{}^{\bar{L}_k}\vec{k}_{\bar{L}_k}$$
 (54)

$${}^{\bar{O}}\omega_{x}{}^{\bar{L}_{k}} = \begin{bmatrix} 0 & 0 & 1 \end{bmatrix}{}^{\bar{L}_{k}} \begin{bmatrix} C \end{bmatrix}^{\bar{O}\bar{O}} [\dot{C}]^{\bar{L}_{k}} \begin{bmatrix} 0 \\ 1 \\ 0 \end{bmatrix}$$
 (55)

$${}^{\bar{O}}\omega_{y}{}^{\bar{L_{k}}} = \begin{bmatrix} 1 & 0 & 0 \end{bmatrix}{}^{\bar{L_{k}}}[C]^{\bar{O}\bar{O}}[\dot{C}]^{\bar{L_{k}}} \begin{bmatrix} 0 \\ 0 \\ 1 \end{bmatrix}$$
 (56)

$${}^{\bar{O}}\omega_z{}^{\bar{L_k}} = \begin{bmatrix} 0 & 1 & 0 \end{bmatrix}{}^{\bar{L_k}}[C]^{\bar{O}\bar{O}}[\dot{C}]^{\bar{L_k}} \begin{bmatrix} 1\\0\\0 \end{bmatrix}$$
 (57)

The angular acceleration vectors of each link and helical drive are calculated from the time derivative of the angular velocity vectors

$$\bar{O}\vec{\alpha}^{\bar{L}_k} = \bar{O}\frac{d}{dt}\bar{O}\vec{\omega}^{\bar{L}_k} \tag{58}$$